IMPACT OF AIR EVACUATION IN OUT-OF-AUTOCLAVE FLOW & COMPACTION MODELING

T. Kourkoutsaki[a *], S. Comas-Cardona[b], C. Binetruy[b], R. K. Upadhyay[c], R. Hinterhölzl[a]

[a] *Institute for Carbon Composites, Technische Universität München, Boltzmannstr. 15, 85478, Garching b. München, Germany*
[b] *Research Institute in Civil Engineering and Mechanics, Ecole Centrale de Nantes, 1 Rue de La Noe, 44321, Nantes, France*
[c] *Composite Technologies, GE Global Research, One Research Circle, Niskayuna, NY 12309, USA*
* *Kourkoutsaki@lcc.mw.tum.de*

Keywords: Out-of-Autoclave, Air evacuation, Gas pressure, Transient flow

Abstract

Due to the partial impregnation and limited pressure available for curing Out-of-Autoclave (OoA) prepreg, modeling the air transport through the tows becomes applicable. Focus is given on predicting the tow fill time for through thickness resin flow taking into account the air evacuation state. This work presents models that can be applied at different stages of the OoA consolidation and cure process, such as models for continuous air extraction, loss of connection with the vacuum source and delayed evacuation.

1. Introduction

1.1. Out of Autoclave processing and process modeling

Composite parts made of prepreg are traditionally cured in the autoclave with application of external pressure. In order to circumvent drawbacks of autoclave manufacturing such as high capital-investment, availability due to increased volumes and part-size constraints, Out-of-Autoclave curing (OoA) was introduced as an alternative in the early 90's [1]. OoA curing is typically taking place in an oven, complemented by a single sided mold, closed under vacuum with a flexible membrane or vacuum bag. The limited pressure available for consolidation (10^5 Pa or 1bar) when compared to Autoclave (approx. 7×10^5 Pa or 7bar) as well as the usage of partially impregnated OoA prepregs [2] can pose a high risk for residual porosity in the finished part if the cure cycle is not optimized to take into account the specific challenges involved. Increased porosity in the manufactured part can lead to a significant deterioration of its mechanical performance as often discussed in literature [3]; among others.

Commercially available OoA prepregs contain a significant amount of air as received from the manufacturer. Due to limited pressure available for Out-of-Autoclave cure, laminate quality cannot be achieved through balancing the hydrostatic and void pressure in order to maintain gas and volatiles in solution, as traditionally performed in autoclave processing [4,5]. In this case the partially dry prepreg allows the vacuum to be evenly distributed throughout the laminate, which becomes the avenue for transporting air, gas and volatiles outside the part. Air flow through the laminate at room temperature and the latency of the matrix during the curing cycle strongly influences the resin-fiber wetting process. Non-optimized curing cycle can cause incomplete wetting of the initially dry regions within the prepreg and lead to porosity formation through air entrapment. The usage of low reactivity thermoset systems assures limited off-gassing during cure [2] suggesting that air entrapment due to incomplete air evacuation of the laminate is the main reason for part porosity.

A few factors affecting the quality of OoA prepreg impregnation and porosity formation are: the length of the part or its distance from the vacuum source [6], the quality of vacuum available during processing [7], material characteristics such as the percentage of initial impregnation within the tow [8, 9], textile architecture and its air permeability [9, 10] as well as resin characteristics such as latency/cure kinetics, affected by heat transfer [2, 8, 11].

Efforts modeling the resin flow in partially impregnated prepregs have been performed using Darcy's Law expressed for single phase flow in a porous medium. The most common approaches are either via applying constant boundary conditions assuming negligible gas entrapment [10], or by including the rate of gas mass flow out of a given part and lay-up [12] later extended to include fiber bed compaction [13]. Another approach available is based on the representation of the OoA prepreg as a two-phase porous media, consisted of a skeleton filled with both air and resin. This continuum mechanics approach aims to couple the preform deformation with the intrinsic fluid pressure and the migrating free surface due to resin infiltration into the fibrous preform [14].

2. Objectives

The aim of this work is the development of a model which would be correlating the air evacuation through the tows of an OoA prepreg with various 'real life' processing scenarios and predicting its impact on tow fill time with resin. The impact of various pressure scenarios present during OoA processing is performed via the application of pressure boundary conditions on the fluid impregnated domain. In this work models for isothermal tow impregnation are developed using this approach based on analytical and numerical solutions implemented in Matlab R2013a.

3. Material and Models

3.1. Material

Figure (1) shows a characteristic cross section of a single tow from the commercially available OoA prepreg Cytec MTM 44-1, based on a 285 g/m^2, 2x2 Twill weave fabric. The picture was taken using optical microscopy (Olympus SXZ10 stereo microscope) after embedding the prepreg in fluorescent resin and polishing.

Figure 1: Characteristic tow morphology for MTM 44-1 prepreg

The tow appears to have of limited initial impregnation, produced by resin film deposition only on one side of the prepreg. The amount of tow wetted through thickness by the resin is relatively small. The exact amount of impregnation within the tow could not be precisely quantified due to the flexible nature of the prepreg at the uncured state, causing focusing issues to the optical microscope used. For this work it is assumed that the resin film is sitting only on the top of the prepreg without impregnating the fibers and thus the pressure drop within this domain is considered to be negligible. The domains wetted by resin are considered fully saturated (s=1) and the non-wetted regions not saturated (s=0). Compaction of the prepreg during impregnation is not taken into account and thus the permeability and porosity of the tow remains constant. A simplified tow of rectangular shape and thickness H_y, consisted solely of unidirectional fibers is selected as the unit cell for further model development (Figure 2).

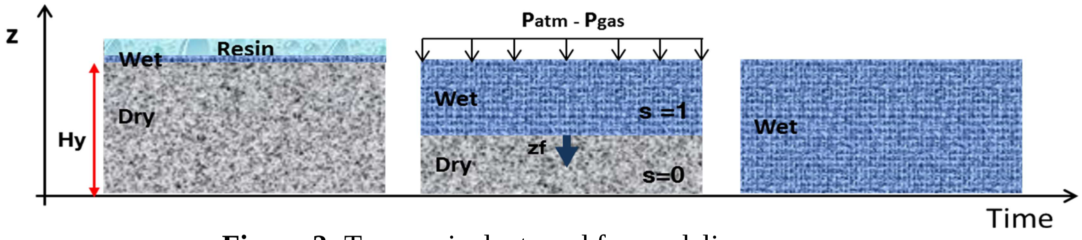

Figure 2: Tow equivalent used for modeling purposes

3.2. Modeling approach

Resin flow through the fiber bed during OoA processing is progressing through the thickness of the tow (z-axis) and since it is a relatively slow process it is modeled at a quasi-steady state. Resin flow is assumed to be incompressible (constant density), which simplifies the conservation of mass into equation (1) and the slow and viscous nature of the fluid flow (i.e. resin in this case) permits the usage of Darcy's law (2).

$$\frac{\partial}{\partial z}(v_D) = 0 \tag{1}$$

$$v_D = -\frac{Kz}{\mu_f}\frac{\partial P_f}{\partial z} \tag{2}$$

Where v_D is Darcy's velocity, Kz the through thickness permeability of the tow, μ_f the viscosity of the fluid and P_f the fluid pressure. By substitution of equation (2) into equation (1) assuming isothermal flow (μ_f, Kz constant), the shape of the liquid pressure profile can be determined from equation (3).

$$\frac{\partial^2 P_f}{\partial z^2} = 0 \rightarrow P_f(z) = Az + B \tag{3}$$

By applying boundary conditions at the initial and flow front positions, the fluid pressure within the impregnated domain can be calculated. More details about the various boundary conditions applied will be given later in the text.

Since Darcy's velocity describes the volume averaged velocity according to equation (4), equation (5) provides the flow front velocity u_f in the porous medium, correlated through its porosity φ.

$$v_D = \langle \varphi u_f \rangle \tag{4}$$

$$u_f = -\frac{Kz}{\varphi\mu_f}\frac{\partial P_f}{\partial z} = -\frac{Kz}{\varphi\mu_f}\frac{\Delta \mathrm{P}}{(Hy - zf)} \tag{5}$$

In order to calculate the time required for filling an area of the tow, equation (5) can be expressed as the rate of change of the flow front position, $\frac{\partial P_f}{\partial z}$ or $\frac{\Delta P}{(Hy - zf)}$ and integrated within the domain of interest. The scenarios of pressure boundary conditions developed are presented in cases 3.2.1 through 3.2.3 below.

3.2.1. Continuous air extraction

This case is referring to the most commonly encountered scenario in liquid composite molding processes, where a constant vacuum pressure $P_{gas} = P_{vac}$ is applied at the resin flow front. The constant pressure difference ΔP between the atmospheric pressure (P_{atm}) and the gas pressure (P_{gas}) is responsible for driving the tow impregnation:

$$\Delta P = P_{atm} - P_{gas} \tag{6}$$

In practice this condition is applicable when an OoA part is connected to the vacuum pump throughout the consolidation and cure process. The theoretical time to fill the complete tow of thickness H_y can be calculated by equation (7).

$$t_{fill} = \frac{\varphi \mu_f}{K_z \Delta P} \frac{{H_y}^2}{2} \tag{7}$$

The resin flow profile (Pf) during impregnation as well as the gas pressure at various flow front positions (zf) and with evolving fill time (t) are presented for this case in Figure (3).

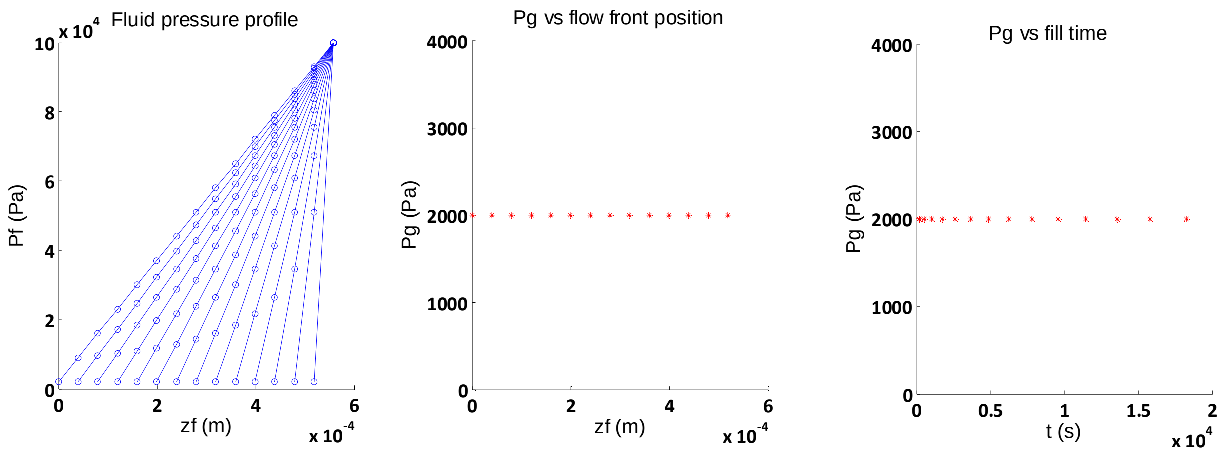

Figure 3: Pressure profiles for tow filling at room temperature based on Case 3.2.1

3.2.2. Loss of connection with the vacuum source

The worst case scenario that can occur during OoA manufacturing is the loss of connection to the vacuum source. In this case a reduced pressure difference is available to drive the prepreg impregnation process.

The gas inside the part is treated in this case as ideal. Hence the ideal gas law equation formulated for gas evolution at constant temperature is used to provide the boundary conditions at the flow front position according to equation (8):

$$P_{gas} V_{gas} = constant \tag{8}$$

Since the gas pressure will increase until it equalizes with atmospheric pressure, the time to impregnate the complete tow is going to increase significantly and will eventually become infinite. For comparison purposes, an analytical expression describing the fill of 96.9% of the complete tow thickness is presented in equation (9):

$$t_{fill_{96.9\%}} = 0.6405 \frac{{H_y}^2 \varphi \mu_f}{K_z P_{atm}} \tag{9}$$

The resin flow profile during impregnation as well as the gas pressure at various flow front positions and with evolving fill time are presented for this case in Figure (4). The gas pressure increases as the liquid flow progresses through the thickness of the tow with evolving fill time. It is important to note that before the complete tow is filled with resin, the gas has equalized with the atmospheric pressure and will not allow complete tow filling. Thus the graph on the right side of Figure (4) represents the gas pressure evolution with fill time, one element before the fill time becomes infinite.

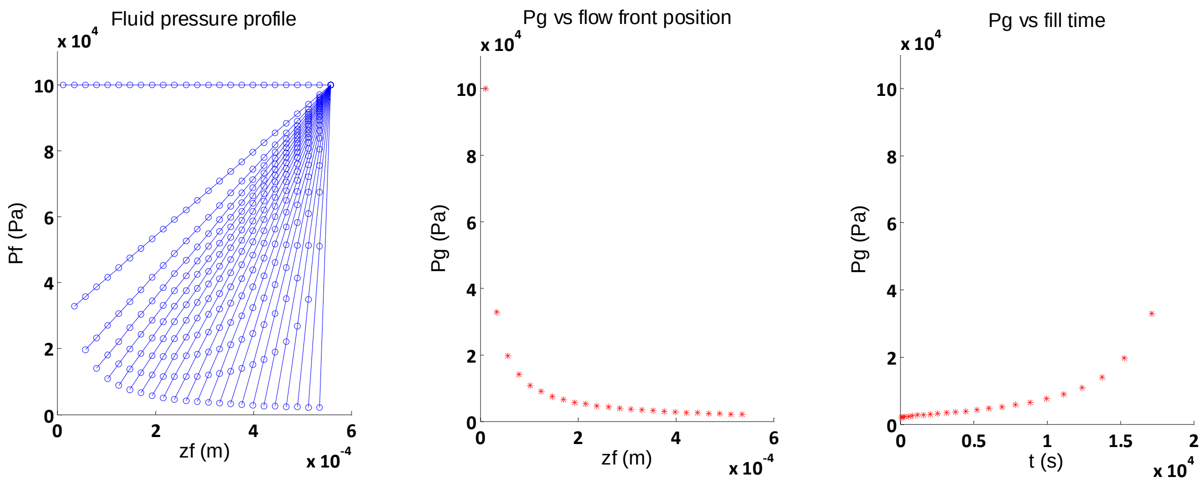

Figure 4: Pressure profiles for tow filling at room temperature based on Case 3.2.2

3.2.3. *Delayed air evacuation*

This scenario is taking into account the air evacuation occurring along the length of a tow, assuming this to be the only path for gas extraction. Equation (10) is used to calculate the gas flow through the fiber tow. This formulation is based on the transient conservation of mass combined with the ideal gas formulation at constant temperature, assuming the gas flow through the fiber bed is Darcian.

$$\frac{\partial P_{gas}}{\partial t} - \frac{K_x}{\varphi \mu_a} \nabla \cdot \left(P_{gas} \nabla P_{gas}\right) = 0 \tag{10}$$

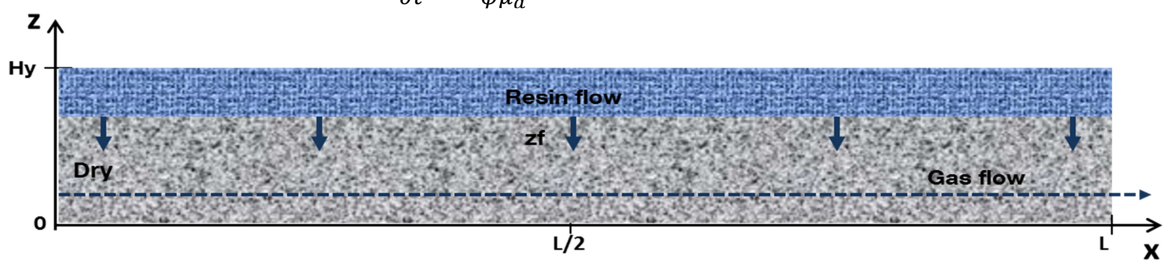

Figure 5: Graphical representation of domain modeled in Case 3.2.2

A similar approach with different boundary conditions has been used by Hou et al. [15] to calculate the in-plane permeability using transient flow. The transient gas flow along the length L of the tow is coupled via gas boundary conditions to the resin flow taking place through the thickness of a tow. This way the fill time of the tow at various positions along the length can vary depending on the gas extraction achieved at the specific time and position. Equation (10) has no known analytical solution. It was solved numerically using the Matlab pdepe function based on the odes15 implicit solver by applying the following initial and boundary conditions:

$$\text{IC:} \quad P_{gas}(x,0) = P_{atm} \qquad \text{BC:} \quad P_{gas}(0,t) = P_{vac} \;\; \& \;\; u\,(L,t) = 0 \Rightarrow \frac{\partial P_{gas}(L,t)}{\partial x} = 0 \qquad (11)$$

The air and fluid flow are coupled weakly within the time frame of transient air evolution. The time frame for the transient evolution of air is derived by the non-dimensionalization of equation (10). The pressure of gas for the first dt is the boundary condition used for the liquid flow initiation. The selection of an appropriate dt for the gas flow as well as a spatial discretization for the fluid flow on z-axis within the time range appropriate for the phenomena is critical for the coupling stability. An example of a resin flow profile during impregnation as well as the gas pressure at various flow front positions and with evolving fill time are presented for this case in Figure (6).

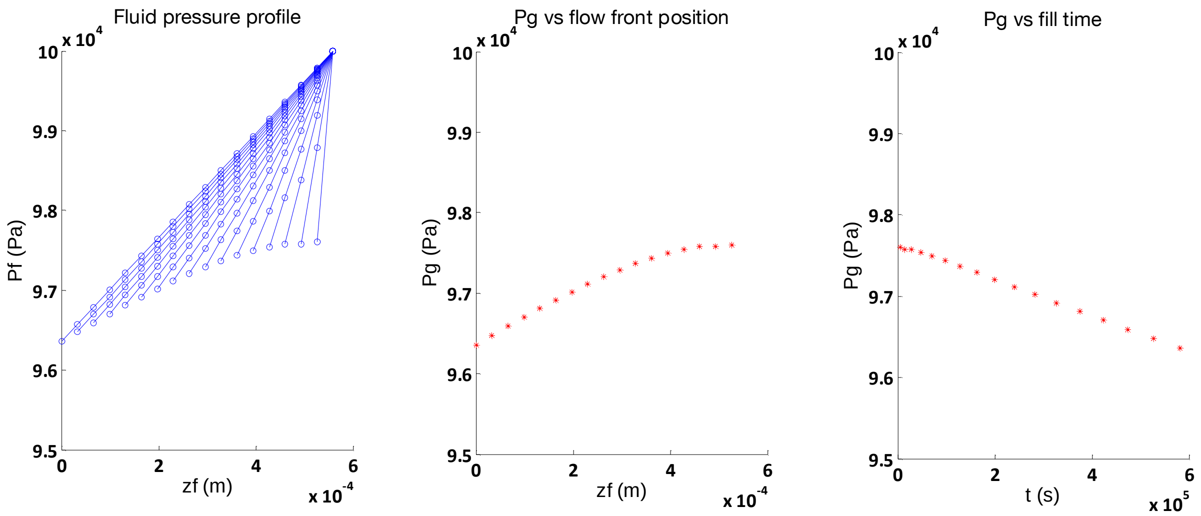

Figure 6: Pressure profiles for tow filling at room temperature based on Case 3.2.3

4. Case study on the influence of part length on tow fill time

In this study the scenario of delayed air evacuation is used to investigate the effect of part length and fluid to gas permeability ratios to the fill time of a single tow. The study is performed under isothermal conditions, at room temperature focusing on the fill time at the mid-span of the tow length (L/2). The coupling between air and resin flow was initiated for all cases at ΔPgas ~2.3%. Input parameters are listed in Table 1. An indicative viscosity of hot-melt epoxies at room temperature is used in the case study. The tow thickness and porosity of the fiber bed is assumed to be constant. A range of in-plane permeability values reported in the literature for various OoA prepregs is used as a basis for this study [9, 12, 16, 17]. The through thickness permeability of OoA prepregs has been measured by Tavares et al. [18]. In order to investigate the effect of a slow flowing gas, a through thickness permeability in the range of 10^{-13} is based on Gebart's equation for transverse flow in the tow is selected [16].

P_{vac} (Pa)	Tow length L (m)	Tow thickness Hy (mm)	μ_a (Pa·s)	μ_f (Pa·s)	K_x (m^2)	K_z (m^2)	φ
2×10^3	0.5	0.559	1.98×10^{-5}	10^4	2.26×10^{-12}	4.68×10^{-13}	0.50
	5.0				5.69×10^{-14}	2.26×10^{-18}	
	10.0				9.60×10^{-15}		
					5.69×10^{-16}		
					2.00×10^{-17}		
					3.00×10^{-18}		

Table 1: Inputs for sensitivity study

The two sub-figures of Figure 7 are reflecting two characteristic material states, a tow less permeable to resin transversely (Figure 7 - left) and a tow less permeable to air longitudinally (Figure 7 - right). Both sub-figures include a region where the tow permeabilities are nearly isotropic ($K_z/K_x\approx1$). If we assume constant through thickness permeability for the resin, coupling transient air flow out of a tow with the resin flow through its thickness can have a significant effect on the tow's fill time. In the case where the longitudinal permeability is lower than the through thickness permeability (Figure 7 - right), increasing tow length and decreasing longitudinal permeability increase significantly the air evacuation time. The decreased air evacuation time is responsible for the delayed filling of the mid-span of the tow with resin. When the through thickness tow permeability is low (Figure 7 - left), the impact of air evacuation is noticeable only for isotropic or nearly isotropic materials. If the longitudinal permeability of the tow becomes a few orders of magnitude lower than the through thickness permeability, the time required to achieve complete air evacuation ($P_{gas} = P_{vac}$) becomes very small comparative to the time required for the resin to flow. In this case the fill time of a tow is independent of length (within the range studied) and approaches the fill time of a tow predicted by the continuous air extraction model. The cases of continuous air extraction (P_g=P_v) and loss of connection with the vacuum source (IGL 96.9% tow) are also plotted for comparison purposes assuming $K_z/K_x\approx1$.

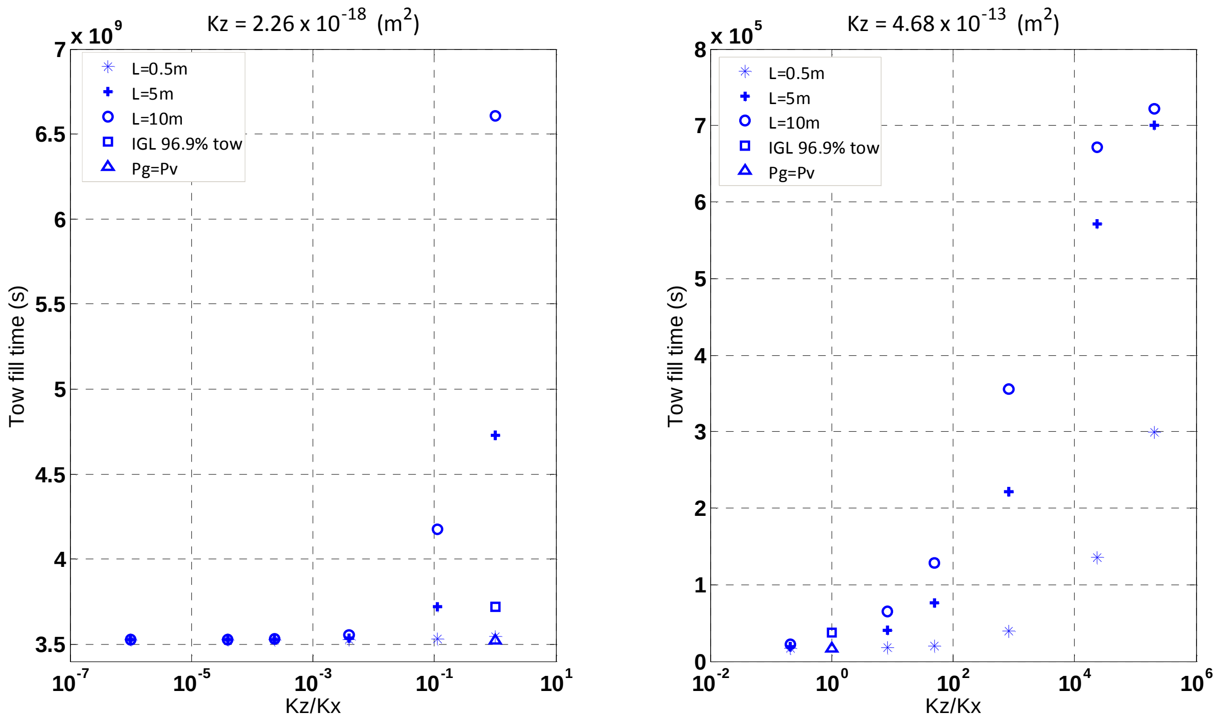

Figure 7: Time to fill a tow of various lengths for various permeability ratios

References

[1] G. Gardiner. Out of Autoclave prepregs: Hype or revolution? *High Performance Composites Magazine*, January 2011.

[2] C. Ridgard. Out of Autoclave Composite Technology for Aerospace, Defense and Space Structures. In *SAMPE '09 Spring Symposium, Baltimore MD*, May 2009.

[3] L. Liu, B.M. Zhang, D. Wang and Z. Wu. Effects of cure cycles on void content and mechanical properties of composite laminates. *Composite Structures*, 73, 303-309, 2006.

[4] J.L. Kardos, M.P. Dudukovic, and R. Dave. Void growth and resin transport during processing of thermosetting matrix composites. In Dusek K., *Epoxy Resins and Composites IV - Advances in Polymer Science* 80, 101-123, Springer-Verlag, July 1986.

[5] F.C. Campbell. In *Manufacturing processes for advanced composites*, Elsevier, New York 2004.

[6] J. Kay and G. Fernlund. Processing Conditions and Voids in Out of Autoclave Prepregs. In *SAMPE '12 Spring Symposium, Baltimore*, May 2012.

[7] T. Centea and P. Hubert. Out-of-autoclave prepreg consolidation under deficient pressure conditions. *Journal of Composite Materials*, 2013.

[8] T. Centea and P. Hubert. Measuring the impregnation of an out-of-autoclave prepreg by micro-CT. *Composites Science and Technology*, 71, 593-599, 2011.

[9] S.B. Shim and J. C. Seferis. Thermal and air permeation properties of a carbon fiber/toughened epoxy based prepreg system. *Journal of Applied Polymer Science*, 65, 5-16, 1997.

[10] T. Centea and P. Hubert. Modelling the effect of material properties and process parameters on tow impregnation in out-of-autoclave prepregs. *Composites Part A: Applied Science and Manufacturing*, 43, 1505-1513, 2012.

[11] J. Kay, L. Fahrhang, K. Hsiao and G. Fernlund. Effect of Process Conditions on Porosity in Out of Autoclave prepreg laminates. In *18th International Conference on Composite Materials*, Jeju Island Korea, August 2011.

[12] G. Fernlund, A. Arafath, and A. Poursartip. Gas Transport in Prepregs: Model and Permeability Experiments. In *17th International Conference on Composite Materials,* Edinburgh, 27-31 July 2009.

[13] R. Helmus, T. Centea, P. Hubert and R. Hinterhoelzl. An Integrated Process Model for Air Evacuation and Tow Impregnation in Out-of-Autoclave Prepreg Consolidation. In *American Society for Composites 28th Technical Conference*, University Park, PA, United States, 9 – 11 September 2013.

[14] M. Wysocki, R. Larsson and S. Toll. Modelling Multiple Scales in Composites Manufacturing. In *10th International Conference on Flow Processes in Composite Materials (FPCM10),* Monte Verita, Ascona,CH, 11-15 July 2010.

[15] Y. Hou, S. Comas-Cardona, C. Binetruy and S. Drapier. Gas transport in fibrous media: Application to in-plane permeability using transient flow. *Journal of Composite Materials*, 47, 22-37 2013.

[16] B. Gebart. Permeability of Unidirectional Reinforcements for RTM. *Journal of Composite Materials*, 26, 1100-1133, 1992.

[17] C.M.D Hickey, J.G. Timms and S. Bickerton. Compaction Response and Air Permeability Characterization of Out-of-Autoclave Prepreg Materials. In *11th International Conference on Flow Processes in Composite Materials (FPCM 11),* Auckland, 9-12 July 2012.

[18] S.S. Tavares, V. Michaud and J.-A.E. Månson. Through thickness air permeability of prepregs during cure. *Composites Part A: Applied Science and Manufacturing*, 40, 1587–1596, 2009.